Article

New Biscoumarin Derivatives: Synthesis, Crystal Structure, Theoretical Study and Antibacterial Activity against *Staphylococcus aureus*

Di Qu [1,†], Jing Li [2,†], Xiao-Hui Yang [2], Zi-Dan Zhang [3], Xiao-Xing Luo [1], Ming-Kai Li [1,*] and Xia Li [4,*]

[1] Department of Pharmacology, School of Pharmacy, the Fourth Military Medical University, Xi'an 710032, China; E-Mails: qudi3157@126.com (D.Q.); xxluo3@fmmu.edu.cn (X.-X.L.)

[2] School of Chemistry and Chemical Engineering, Xi'an University, Xi'an 710065, China; E-Mails: lijing_518@126.com (J.L.); yangxh1127@aliyun.com (X.-H.Y.)

[3] Department of Physics, School of Science, Tianjin University, Tianjin 300072, China; E-Mail: zhangzidan@tju.edu.cn

[4] Department of Neurosurgery, Xijing Hospital, the Fourth Military Medical University, Xi'an 710032, China

[†] These authors contributed equally to this work.

[*] Authors to whom correspondence should be addressed; E-Mails: mingkai@fmmu.edu.cn (M.-K.L.); sjwklixia@sina.com (X.L.); Tel./Fax.: +86-29-8477-4555 (M.-K.L.); +86-29-8477-5539 (X.L.).

Abstract: Five novel biscoumarins **1**–**5** were synthesized and characterized. In these compounds, two classical asymmetrical intramolecular O–H⋯O hydrogen bonds were used to stabilize the whole structures and the HB energies were performed with the density functional theory (DFT) [B3LYP/6-31G*] method. The five compounds were evaluated for their *in vitro* antibacterial activities against *Staphylococcus aureus* (*S. aureus* ATCC 29213), methicillin-resistant *S. aureus* (MRSA XJ 75302), vancomycin-intermediate *S. aureus* (Mu50 ATCC 700699), and USA 300 (Los Angeles County clone, LAC) by the means of minimum inhibitory concentration and time-kill curves.

Keywords: biscoumarin; *Staphylococcus aureus*; minimum inhibitory concentration
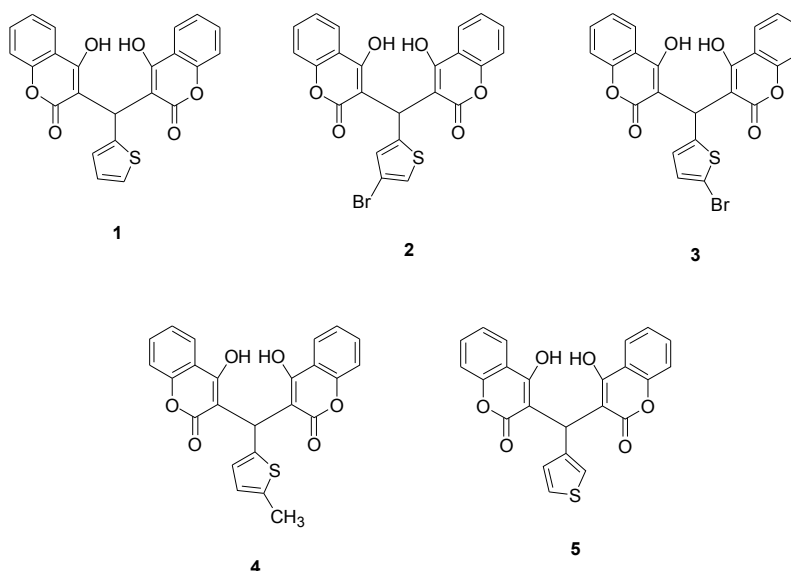
1. Introduction

Staphylococcus aureus (*S. aureus*) is a major pathogen, and the leading cause of healthcare-associated infections [1]. It can cause severe sepsis complicated by acute renal failure and respiratory failure requiring intensive care [2,3]. However, many strains of which are now resistant to almost all the antibiotics. Naturally occurring strains of methicillin-resistant *Staphylococcus aureus* (MRSA) were first reported in England in 1961 [4], not long after the introduction of semisynthetic penicillins. The prevalence rates of MRSA in hospitals in some Asian countries, such as Taiwan, China, Japan, and South Korea, range from 70% to 80% [5,6]. Because the efficacy of novel therapeutic agents against MRSA stays largely unexplored, the treatment failure of MRSA infections makes this field be of great interest in the future.

4-Hydroxycoumarin derivatives have attracted much interest in several fields and represent an important class of organic heterocycles that can be found in many natural or synthetic drugs [7–9]. These compounds possess versatile biological activities, such as anticoagulant, insecticidal, antihelminthic, hypnotic, and antifungal activities, phytoalexin production, and HIV protease inhibition [10–13]. Biscoumarins consisting of a 4-hydroxycoumarin dimer have received considerable attention because of their special molecular structures (two intramolecular O–H···O hydrogen bonds) and diverse biological properties through chemical modifications (different substituents on the central linker methylene). Recognizing the considerable importance of the compounds, the researchers focused on the synthesis of biscoumarin derivatives.

In the current study, a series of biscoumarins (Figure 1), namely, 3,3'-(2-thienyl-methylene)-bis-(4-hydroxycoumarin) (**1**), 3,3'-(4-bromo-2-thienyl-methylene)-bis-(4-hydroxycoumarin) (**2**), 3,3'-(5-bromo-2-thienylmethylene)-bis-(4-hydroxycoumarin) (**3**), 3,3'-(5-methyl-2-thienylmethylene)-bis-(4-hydroxycoumarin) (**4**) and 3,3'-(3-thienyl-methylene)-bis-(4-hydroxycoumarin) (**5**), were synthesized and their antibacterial activities were investigated in detail. A possible relationship between such hydrogen-bonded structures and their antibacterial activities was further studied by theoretical calculations.

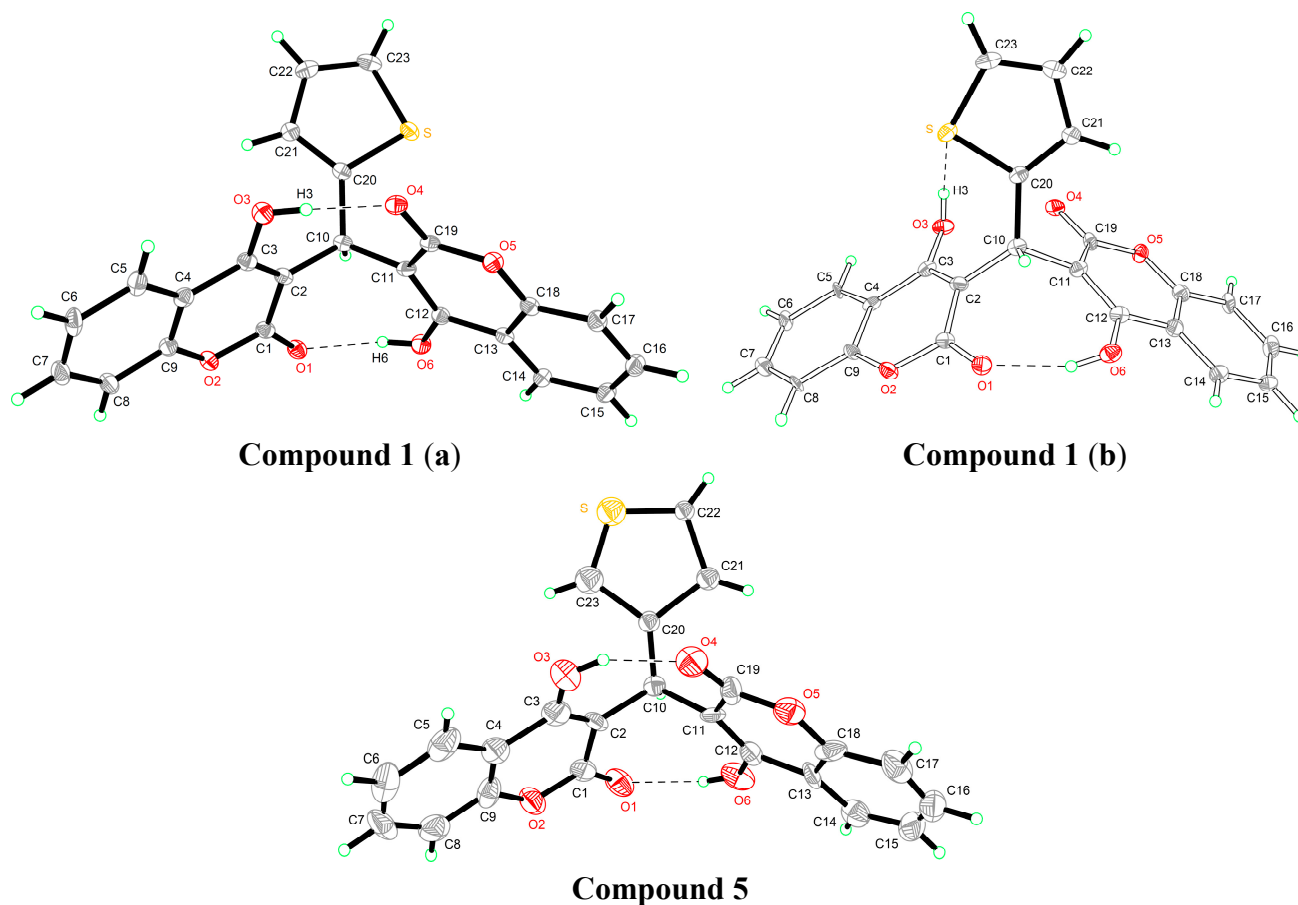**Figure 1.** Chemical structures of compounds **1**–**5**.

2. Results and Discussion

2.1. Molecular Structure

The crystal structures of compounds **1** and **5** are given in Figure 2. In the crystal structure of compound **1**, two crystallographically independent molecules are present in the asymmetric unit. The whole molecule is disordered over two orientations with refined site occupancies of 0.75:0.25, and two 4-hydroxycoumarin fragments are linked by a methylene bridge, wherein one hydrogen atom is replaced with a 2-thienyl residue. However, the two components differ with respect to the reversed twist directions of two 4-hydroxycoumarin molecules. In the major component (a), two classical intramolecular hydrogen bonds were found; each links a coumarin hydroxyl and carbonyl group [d(O$_3$–O$_4$) = 2.592 Å, d(O$_1$–O$_6$) = 2.697 Å]. In the minor component (b), one classical intramolecular hydrogen bond is between a hydroxyl group of one coumarin fragment and a lactone carbonyl group of another coumarin fragment; the other classical intramolecular hydrogen bond is between a hydroxyl group of one coumarin fragment and thiophene ring S atom.

Like compound **1**, in the crystal structure of compound **5**, two 4-hydroxycoumarin moieties are linked through a methylene bridge, wherein one hydrogen atom has been replaced with a 3-thienyl residue. In addition, two classical asymmetrical intramolecular O–H···O hydrogen bonds [d(O$_3$–O$_4$) = 2.587 Å, d(O$_1$–O$_6$) = 2.709 Å] between two 4-hydroxycoumarin fragments were used to stabilize the whole structure.

Figure 2. Crystal structures of compounds **1** and **5**.

Compound 1 (a)

Compound 1 (b)

Compound 5

2.2. Quantum Chemical Calculations

2.2.1. Geometric Parameters of Compounds **1**–**5**

The fully optimized molecular structures of compounds **1**–**5** with atomic numbering calculated at B3LYP level of theory are shown in Figure 3. Selected calculated geometric parameters under three different basis sets (6-31G*, 6-31+G**, and 6-311G*) and experimental geometric parameters of compounds **1** and **5** are presented in Table 1.
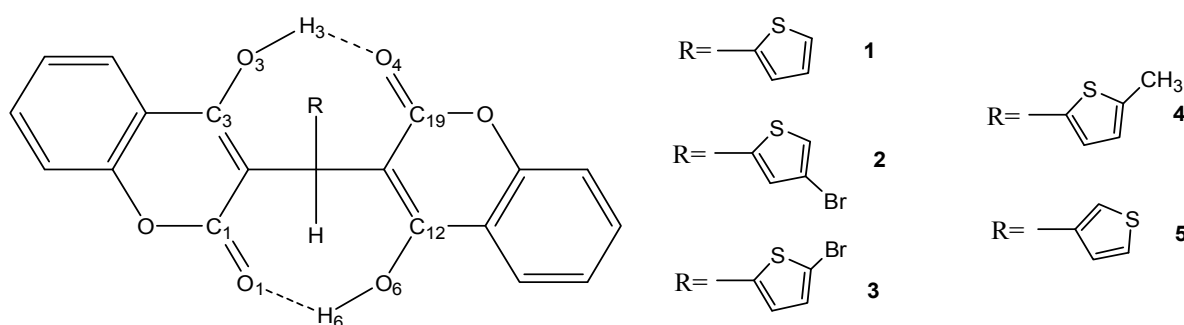
Figure 3. Schematic representation of compounds **1**–**5**.

Table 1. Experimental and calculated parameters of the selected bond lengths and bond angles of compounds **1** and **5**.

Name Definition	Compound 1				Compound 5			
	X-ray	6-31G*	6-31+G**	6-311G*	X-ray	6-31G*	6-31+G**	6-311G*
$O_3 \cdots O_4$	2.592	2.639	2.614	2.643	2.587	2.643	2.621	2.648
$O_1 \cdots O_6$	2.697	2.704	2.695	2.711	2.709	2.698	2.686	2.706
$C_{19}=O_4$	1.234	1.229	1.232	1.222	1.192	1.229	1.232	1.222
$C_1=O_1$	1.235	1.233	1.236	1.226	1.214	1.233	1.236	1.226
C_1-O_2	1.361	1.372	1.370	1.371	1.309	1.373	1.371	1.372
C_9-O_2	1.355	1.367	1.369	1.366	1.324	1.368	1.369	1.366
$C_{19}-O_5$	1.352	1.376	1.373	1.375	1.318	1.377	1.375	1.377
$C_{18}-O_5$	1.354	1.367	1.368	1.365	1.389	1.367	1.368	1.365
$C_{10}-C_{20}$	1.514	1.521	1.522	1.520	1.412	1.529	1.529	1.528
$C_1-C_2-C_{10}$	113.63	114.14	114.12	113.94	113.38	114.62	114.65	114.40
$C_3-C_2-C_{10}$	126.92	126.33	126.55	126.52	126.59	125.76	125.91	125.96
$C_{10}-C_{11}-C_{19}$	119.17	118.92	119.07	118.71	115.55	119.12	119.37	118.90
$C_{10}-C_{11}-C_{12}$	122.30	121.42	121.47	121.58	127.08	121.40	121.37	121.56
$C_2-C_{10}-C_{11}$	112.56	113.41	113.58	113.51	110.78	112.96	113.15	113.03
$C_2-C_{10}-C_{20}$	116.66	114.66	114.89	114.82	114.91	114.48	114.43	114.59
$C_{11}-C_{10}-C_{20}$	111.34	113.97	114.02	113.95	115.93	115.02	115.38	115.01
$C_3-C_2-C_{10}-C_{11}$	84.78	83.91	83.52	84.56	88.12	87.60	87.46	88.20
$C_2-C_{10}-C_{11}-C_{19}$	82.36	83.36	83.13	83.08	87.43	81.07	80.59	80.82
$C_1-C_2-C_{10}-C_{20}$	136.87	134.30	133.69	134.30	134.62	135.07	134.21	135.02
$C_{19}-C_{11}-C_{10}-C_{20}$	50.79	50.27	51.08	50.88	45.85	52.90	53.89	53.37

The values under three different basis sets are very close, and the calculated results agree with the experimental findings. The average discrepancy of the selected bond lengths and bond angles between

theoretical and experimental data is less than ±0.02 Å and ±2°, respectively. B3LYP/6-31G* exhibited sufficient agreement with experimental data and lower computational cost, so further theoretical study was performed at this level.

2.2.2. Estimation of the Single and Total HB Energies in Compounds **1**–**5**

To obtain single and total HB energies of the five compounds, structure optimization was performed to elucidate stable PES structures. We take compound **5** as an example to estimate single and total HB energies. Compound **5** which was stabilized by two HBs is the global minimum structure (**5ab**); however, there also could be two higher energy structures (**5a** and **5b**) stabilized by one HB respectively.

The O_6—$H_6 \cdots O_1$ HB energy was estimated from the energy difference between **5ab** and **5a**, $E(O_6$—$H_6 \ldots O_1) = E_{5ab}^{coor} - E_{5a}^{coor}$, calculated to be −50.56713 kJ/mol (Table 2). **5a** is a global minimum structure with one HB (O_3—$H_3 \cdots O_4$). The O_3—$H_3 \cdots O_4$ HB energy was estimated from the energy difference between **5ab** and **5b**, $E(O_3$—$H_3 \ldots O_4) = E_{5ab}^{coor} - E_{5b}^{coor}$, calculated to be −65.4615915 kJ/mol (Table 2). **5b** was obtained from the global minimum structure of **5ab**, but H_3 was rotated around the C_3—O_3 bond until O_3—$H_3 \cdots O_4$ HB rupture occurred. From the above HB energies values, we can see that O_3—$H_3 \cdots O_4$ HB strength is stronger than that of O_6—$H_6 \cdots O_1$, which is consistent with the fact that the distance of O_3—O_4 (2.587 Å) is shorter than that of O_6—O_1 (2.709 Å). The total HB energy in compound **5**, calculated by the equation $2E_{5ab}^{coor} - (E_{5a}^{coor} + E_{5b}^{coor})$, was estimated to be −116.0287215 kJ/mol (Table 2). Like compound **5**, the O_3—$H_3 \cdots O_4$ HB energy for compounds **1**–**4** is also stronger than O_6—$H_6 \cdots O_1$ HB energy. In addition, the total HB energies of compounds **1**–**4** are −125.4805215, −122.274786, −123.529775, −126.743387 kJ·mol^{-1}, respectively (Table 2).

Table 2. Total electronic energies (in Hartree) and HB energies (in kJ/mol) of hydrogen bonded conformers of compounds **1**–**5** calculated at B3LYP/6-31G* level of theory.

System	Total Electronic Energies [a]	E(O_6—$H_6 \cdots O_1$)	E(O_3—$H_3 \cdots O_4$)	E(Total HB)
1ab	−1734.116678			−125.4805215
1a	−1734.096324	−53.439427		
1b	−1734.089239		−72.0410945	
2ab	−4305.229694			−122.274786
2a	−4305.209554	−52.87757		
2b	−4305.203262		−69.397216	
3ab	−4305.225972			−123.529775
3a	−4305.206014	−52.399729		
3b	−4305.19888		−71.130046	
4ab	−1773.408037			−126.743387
4a	−1773.387526	−53.8516305		
4b	−1773.380274		−72.8917565	
5ab	−1734.116974			−116.0287215
5a	−1734.097714	−50.56713		
5b	−1734.092041		−65.4615915	

[a]: ZP corrected.

2.3. Minimal Inhibitory Concentration (MIC) Assay

Four *S. aureus* bacterial strains, including one drug-sensitive *S. aureus* (*S. aureus* ATCC 29213) strain and three MRSA strains (MRSA XJ 75302, Mu50, USA 300 LAC), were used in the systematic analysis of the antibacterial activities of compounds **1**–**5** *in vitro*. As shown in Table 3, among the compounds, compound **1** exerted the most potent bactericidal effects against nearly all types of *S. aureus* tested, and its MIC values ranged from 8 to 32 μg/mL. By contrast, the other compounds exerted weaker bactericidal effects against *S. aureus*, and their MIC values exceed 32 μg/mL for *S. aureus* (ATCC 29213) and the three MRSA strains. Compared with the MIC values of the above compounds, the MIC values of ceftazidime, ceftriaxone, gentamicin and piperacillin against *S. aureus* (ATCC 29213) strains were lower (less than 8 μg/mL) but were higher against resistant strains at varying degrees.

Table 3. MIC of compounds **1**–**5** and antibiotics in Mueller-Hinton Broth Culture.

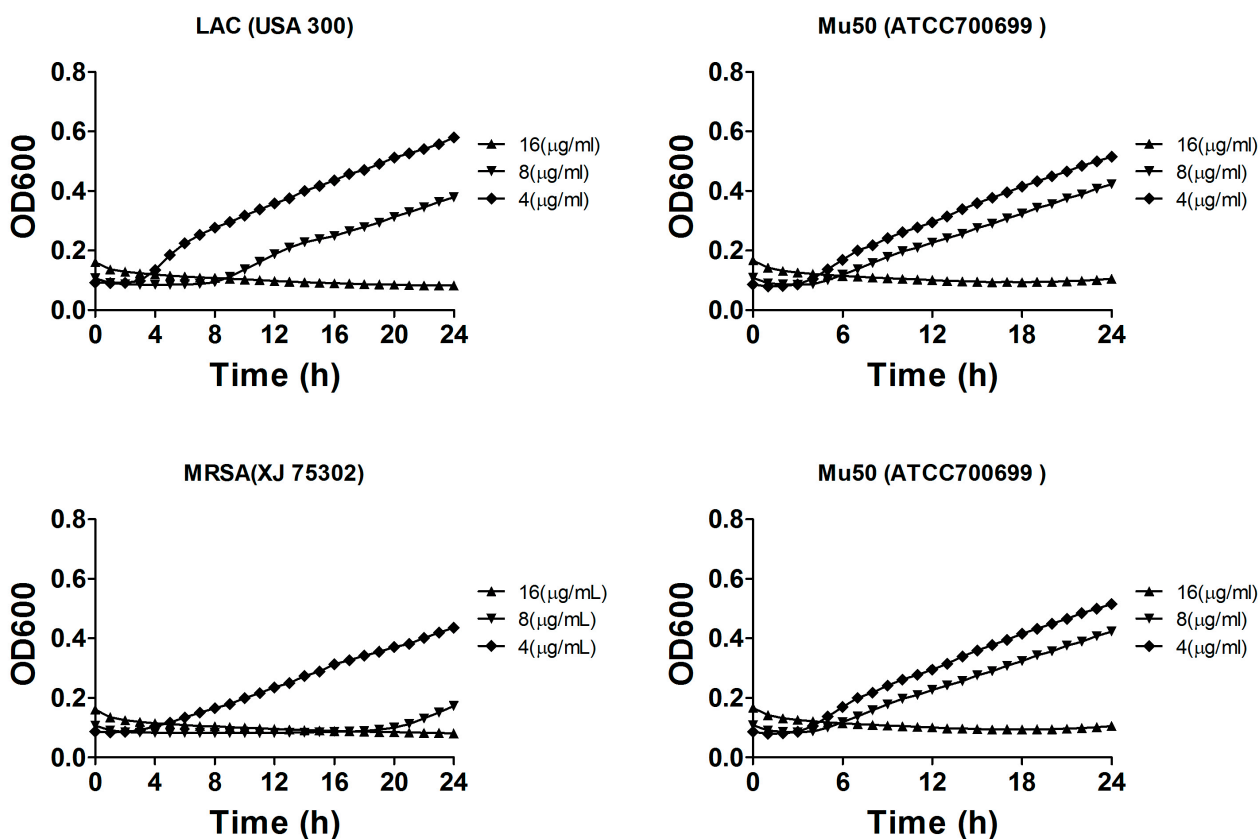| Drug	MIC (ug/mL)			
	S. aureas (ATCC 29213)	MRSA (XJ 75302)	Mu50 (ATCC 700699)	LAC (USA 300)
Compound **1**	8	8	16	32
Compound **2**	64	64	64	128
Compound **3**	64	64	64	128
Compound **4**	32	32	32	32
Compound **5**	>256	>256	>256	>256
Ceftazidime	8 (S)	>256 (R)	256 (R)	64 (R)
Ceftriaxone	2 (S)	>256 (R)	256 (R)	32 (R)
Gentamicin	0.12 (S)	64 (R)	32 (R)	0.25 (S)
Piperacillin	2 (S)	>128 (R)	>128 (R)	64 (R)

S means drug susceptibility; R means drug resistance. Ceftazidime, ceftriaxone, gentamicin, and piperacillin as control antibiotics exert anti-bacterial effects on the drug-susceptible *S. aureas* strain (ATCC 29213). MRSA (XJ 75302) and Mu50 (ATCC 700699) are resistant to all of the control antibiotics, whereas LAC (USA 300) is susceptible to gentamicin but resistant to the other control antibiotics.

2.4. Bacterial Growth Inhibition

We further investigated the growth inhibitory and bactericidal effects to gain insight into the mode of action of compound **1**. Additional experiments were performed to determine the growth rate of *S. aureus* in liquid medium containing the different concentrations of the compound. Compound **1** was added to cultures at concentrations of 4, 8 or 16 μg/mL to evaluate the growth inhibitory effects on *S. aureus* ATCC 29213, MRSA XJ 75302, Mu50, and MRSA USA 300 LAC. As shown in Figure 4, compound **1** inhibited the growth of these pathogens and exhibited almost completely growth inhibition on these pathogens at 8 or 16 μg/mL. Similar to the results of the MIC values, the other compounds hardly showed any inhibitory effects on these pathogens at these concentrations (data was not shown). *S. aureus* growth in MH broth without any compounds, which was used as the control sample, did not exhibit any significant growth inhibitory effect. The analysis of bacterial growth

inhibition showed that aside from exerting antibacterial activities on *S. aureus,* compound **1** also inhibited the growth of the drug-sensitive and drug-resistant *S. aureus* strains.

Figure 4. Concentration-dependent inhibition of compound **1** on the growth of *S. aureus* ATCC 29213, MRSA XJ 75302, Mu50, and MRSA USA 300 LAC. The cells were cultured in liquid culture medium and treated with different concentrations of compound **1**.

3. Experimental Section

3.1. Apparatus and Materials

IR spectra (400–4000 cm^{-1}) were obtained using a Bruker Equinox-55 spectrophotometer. ^{1}H-NMR spectra were obtained (at 400 MHz) using a Varian Inova-400 spectrometer. Mass spectra were obtained using a micrOTOF-Q II mass spectrometer. The melting points were taken on a XT-4 micro melting apparatus, and the thermometer was uncorrected. All antibiotics used were purchased from the National Institute for the Control of Pharmaceutical and Biological Products (Beijing, China). All other chemicals and solvents were of analytical grade. MRSA (XJ 75302) was isolated from cultures of sputum samples from patients in Xijing Hospital (Xi'an, China). *S. aureus* strain (ATCC 29213) was purchased from the Chinese National Center for Surveillance of Antimicrobial Resistance. Mu50 (ATCC 700699) and USA 300 (LAC) were purchased from MicroBiologics (Saint Cloud, MN, USA).

3.2. Synthesis and Characterization of Compounds 1–5

Compounds **1**–**5** were synthesized according to the methods of a previous report [14]. A mixture of thiophene-2-carbaldehyde (or 4-bromo-thiophene-2-carbaldehyde, 5-bromo-thiophene-2-carbaldehyde, 5-methyl-thiophene-2-carbaldehyde and thiophene-3-carbaldehyde) (10 mmol) and 4-hydroxycoumarin (20 mmol) was dissolved in EtOH (100 mL). A few drops of piperidine were added, and the mixture was stirred for 3 h at room temperature. After reaction completion as determined by TLC, water was added until precipitation occurred. After filtering the precipitates, they were sequentially washed with ice-cooled water and ethanol and then dried under vacuum.

3,3′-(2-Thienyl-methylene)-bis-(4-hydroxycoumarin) (**1**): m.p. 206–207 °C. IR (KBr pellet cm^{-1}): 1665, 1612, 1567, 1514, 1356, 767 cm^{-1}. ^{1}H-NMR (CDCl$_3$, δ, ppm): 11.803 (s, 1H), 11.290 (s, 1H), 8.017–8.073 (m, 2H), 7.617–7.656 (q, 2H), 7.399–7.420 (d, 4H), 7.214–7.227 (d, 1H), 6.940–6.962 (t, 1H), 6.855–6.864 (t, 1H), 6.200 (s, 1H). HRMS (ESI$^+$): *m/z*: calcd. for C$_{23}$H$_{14}$SO$_6$: 441.0403 [M+Na$^+$]; found: 441.0411.

3,3′-(4-Bromo-2-thienyl-methylene)-bis-(4-hydroxycoumarin) (**2**): m.p. 207–208 °C. IR (KBr pellet cm^{-1}): 1666, 1620, 1571, 1533, 1363, 1246, 1143, 911, 760 cm^{-1}. ^{1}H-NMR (CDCl$_3$, δ, ppm): 11.871 (s, 1H), 11.307 (s, 1H), 8.045–8.090 (t, 2H), 7.651–7.690 (t, 2H), 7.422–7.443 (d, 4H), 7.144 (s, 1H), 6.789 (s, 1H), 6.169 (s, 1H). HRMS (ESI$^+$): *m/z*: calcd. for C$_{23}$H$_{13}$BrO$_6$S: 518.9508 [M+Na$^+$]; found: 518.9532.

3,3′-(5-Bromo-2-thienyl-methylene)-bis-(4-hydroxycoumarin) (**3**): m.p. 217–218 °C. IR (KBr pellet cm^{-1}): 1673, 1620, 1552, 1492, 1356, 1318, 1205, 1099, 971, 767 cm^{-1}. ^{1}H-NMR (CDCl$_3$, δ, ppm): 11.890 (s, 1H), 11.299 (s, 1H), 8.036–8.090 (q, 2H), 7.646–7.685 (t, 2H), 7.420–7.441 (d, 4H), 6.910–6.919 (d, 1H), 6.634–6.647 (q, 1H), 6.118–6.122 (d, 1H). HRMS (ESI$^+$): *m/z*: calcd. for C$_{23}$H$_{13}$BrO$_6$S: 518.9508 [M+Na$^+$]; found: 518.9589.

3,3′-(5-Methyl-2-thienyl-methylene)-bis-(4-hydroxycoumarin) (**4**): m.p. 209–210 °C. IR (KBr pellet cm^{-1}): 1673, 1605, 1567, 1492, 1363, 1311, 1265, 1212, 1107, 767 cm^{-1}. ^{1}H-NMR (CDCl$_3$, δ, ppm): 11.828 (s, 1H), 11.279 (s, 1H), 8.062 (s, 2H), 7.628–7.667 (t, 2H), 7.389–7.432 (t, 4H), 6.608–6.644 (d, 2H), 6.160 (s, 1H), 2.438 (s, 3H). HRMS (ESI$^+$): *m/z*: calcd. for C$_{24}$H$_{16}$SO$_6$: 455.0560 [M+Na$^+$]; found: 455.0599.

3,3′-(3-Thienyl-methylene)-bis-(4-hydroxycoumarin) (**5**): m.p. 226–227 °C. IR (KBr pellet cm^{-1}): 1661, 1600, 1539, 1521, 1349, 1240, 1090, 910, 760 cm^{-1}. ^{1}H-NMR (CDCl$_3$, δ, ppm): 11.584 (s, 1H), 11.308 (s, 1H), 8.023–8.093 (q, 2H), 7.631–7.670 (q, 2H), 7.418–7.436 (d, 4H), 7.306–7.325 (q, 1H), 7.037 (s, 1H), 6.890–6.902 (d, 1H), 5.986 (s, 1H). HRMS (ESI$^+$): *m/z*: calcd. for C$_{23}$H$_{14}$SO$_6$: 441.0403 [M+Na$^+$]; found: 441.0465.

3.3. X-ray Crystallography

For X-ray diffraction experiments, single crystals of compounds **1** and **5** were both grown from methanol. The X-ray diffraction data were collected on a Bruker SMART APEX II CCD

diffractometer equipped with a graphite monochromated Mo Kα radiation ($\lambda = 0.71073$ Å) by using the ω-2θ scan technique at room temperature. The structure was solved by direct methods using SHELXS-97 [15] and refined using the full-matrix least squares method on F^2 with anisotropic thermal parameters for all non-hydrogen atoms by using SHELXL-97. Hydrogen atoms were generated geometrically. The crystal data and details concerning data collection and structure refinement are given in Table 4. Molecular illustrations were prepared using the XP package. Parameters in CIF format are available as Electronic Supplementary Publication from Cambridge Crystallographic Data Centre.

Table 4. Crystal data, data collection and structure refinement.

Parameter	Compound 1	Compound 5
Formula	$C_{23}H_{14}O_6S$	$C_{23}H_{14}O_6S$
Mr	418.40	418.40
Temperature/K	113(2)	293(2)
Crystal system	Monoclinic	Monoclinic
Space group	$P2_1/n$	$P2_1/n$
a/Å	7.7250(8)	7.7983(4)
b/Å	8.9250(10)	8.9785(5)
c/Å	26.537(2)	26.6473(19)
α/°	90	90
β/°	96.319(9)	96.514(6)
γ/°	90	90
V/Å^3	1818.5(3)	1853.72(19)
Z	4	4
D_{calc}/g·cm^{-3}	1.528	3.009
μ(Mo Kα)/mm^{-1}	1.951	1.711
θ range/°	3.35 to 72.59	2.40 to 25.00
Reflections collected	15733	6656
No. unique data[R(int)]	3541[0.0619]	3261[0.0307]
No. data with $I \geq 2\sigma(I)$	3242	1892
R_1	0.0603	0.2049
ωR_2(all data)	0.1362	0.6273
CCDC	889260	1014707

3.4. Quantum Chemical Calculations

All calculations were carried out using the Gaussian 09 package [16]. Density functional theory (DFT) [17,18], Becke's three-parameter hybrid function (B3LYP) [19], and LYP correlation function [20,21] were used to fully optimize all the geometries on the energy surface without constraints. To obtain precise results that are in conjunction with experimental results, three basis sets, namely 6-31G*, 6-31+G**, and 6-311G*, were tested. Frequency calculations at the B3LYP (with basis sets 6-31G*) level of theory were carried out to confirm stationary points as minima and to obtain the zero-point energies and the thermal correlation data at 1 atm and 298 K.

3.5. Minimal Inhibitory Concentration (MIC) Assay

Based on the CLSI broth microdilution method [22], the determination of minimum inhibitory concentrations (MICs) via microdilution assay was performed in sterilized 96-well polypropylene microtiter plates (Sigma–Aldrich, St. Louis, MO, USA) in a final volume of 200 μL. Bacteria were grown overnight in nutrient broth. Mueller–Hinton (MH) broth (100 μL) containing bacteria (5×10^5 CFU/mL) was added to 100 μL of the culture medium containing the test compound (0.12 μg/mL to 256 μg/mL in serial twofold dilutions). The plates were incubated at 37 °C for 20 h in an incubator. About 50 μL of 0.2% triphenyl tetrazolium chloride (TTC), a colorimetric indicator, was added to each well of microtiter plates and incubated at 35 °C for 1.5 h. The TTC-based MIC was determined as the lowest concentration of oxacillin that showed no red color change indicating complete growth inhibition.

3.6. Bacterial Growth Inhibition

To obtain the time–kill curves for methicillin-susceptible *S. aureus* and MRSA, the synthetic compounds and antibiotics were added to strain cultures to a final concentration of 4, 8 or 16 μg/mL [23]. The strains were cultivated in the automated Bioscreen C system (Lab Systems, Helsinki, Finland) by using an MH broth culture medium. The working volume in the wells of the Bioscreen plate was 300 μL, which comprised 150 μL of the MH broth and 150 μL of the drug solution. The temperature was controlled at 35 °C, and the optical density of the cell suspensions was measured automatically at 600 nm in regular intervals of 10 min for 20 h. Before each measurement, the culture wells were automatically shaken for 60 s. Statistical data for each experiment were obtained from at least two independent assays performed in duplicate.

4. Conclusions

The emergence of vancomycin-resistant *S. aureus* and treatment failure of MRSA infections urgently requires developing new antimicrobials [24–26]. In the current work, we report the synthesis, crystal structures, and antibacterial of the novel biscoumarin derivatives, and observed their activity on clinical isolates strains including methicillin-susceptible or methicillin-resistant *S. aureus*. Both MICs and bacterial growth inhibition results showed that compound **1** exerted potent bactericidal effects against almost all *S. aureus* tested including the MRSA.

Two intramolecular O—H···O HBs in the five compounds were considered as an important factor for biological activity by assisting the molecule to attain the correct configuration. The calculated results are creditable because of the fully optimized molecular structures of compounds **1** and **5** calculated at B3LYP level of the theory using three different basis sets (6-31G*, 6-31+G** and 6-311G*) were in agreement with their available X-ray data.

The total HB stabilization energies in compounds **1–4** were estimated to be −125.4805215, −122.274786, −123.529775 and −126.743387 kJ/mol, which is higher than that of compound **5** (−116.0287215 kJ/mol). These values suggest that the most potent antibacterial activity of compound **1** is basically consistent with the stronger HB strengths. Additional experiments should be carried out to further define the mechanism underlying its anti-bacterial activity and evaluate the correlations of its drug efficacy *in vivo*.

Acknowledgments

Author Contributions

Di Qu performed the MICs and bacterial growth inhibition experiments; Jing Li and Xiao-Hui Yang synthesized and characterized the compounds; Zi-Dan Zhang did the quantum chemical calculations; Ming-Kai Li and Xiao-Xing Luo designed the study and prepared the manuscript; Xia Li was principle investigator of the project and provided the research funding.

Conflicts of Interest

The authors declare no conflict of interest.

References

1. Taylor, A.R. Methicillin-resistant Staphylococcus aureus infections. *Prim. Care* **2013**, *40*, 637–654.
2. Xia, J.; Gao, J.; Kokudo, N.; Hasegawa, K.; Tang, W. Methicillin-resistant *Staphylococcus aureus* antibiotic resistance and virulence. *Biosci. Trends* **2013**, *7*, 113–121.
3. Pottinger, P.S. Methicillin-resistant Staphylococcus aureus infections. *Med. Clin. North Am.* **2013**, *97*, 601–619.
4. Barber, M. Methicillin-resistant staphylococci. *J. Clin. Pathol.* **1961**, *14*, 385–393.
5. Tarai, B.; Das, P.; Kumar, D. Recurrent challenges for clinicians: Emergence of methicillin-resistant *Staphylococcus aureus*, vancomycin resistance, and current treatment options. *J. Lab. Phys.* **2013**, *5*, 71–78.
6. Hetem, D.J.; Bonten, M.J. Clinical relevance of mupirocin resistance in *Staphylococcus aureus*. *J. Hosp. Infect.* **2013**, *85*, 249–256.
7. Cravotto, G.; Nano, G.M.; Palmisano, S.G.; Tagliapietra, S. The chemistry of coumarin derivatives. Part XIII. The reactivity of 4-hydroxycoumarin under heterogeneous high-intensity sonochemical conditions. *Synthesis* **2003**, *8*, 1286–1291.
8. Atta-ur-Rahman; Shabbir, M.; Ziauddin Sultani, S.; Jabbar, A.; Choudhary, M.I. Cinnamates and coumarins from the leaves of Murraya paniculata. *Phytochemistry* **1997**, *44*, 683–685.
9. Al-Amiery, A.A.; Al-Bayati, R.I.H.; Saour, K.Y.; Radi, M.F. Cytotoxicity, antioxidant, and antimicrobial activities of novel 2-quinolone derivatives derived from coumarin. *Res. Chem. Intermed.* **2012**, *38*, 559–569.
10. Kontogiorgis, C.; Hadjipavlou-Litina, D. Biological evaluation of several coumarin derivatives designed possible anti-inflammatory/antioxidant agents. *J. Enzym. Inhib. Med. Chem.* **2003**, *18*, 63–69.
11. Smyth, T.; Ramachandran, V.N.; Smyth, W.F. A study of the antimicrobial activity of naturally occurring and synthetic coumarins. *Int. J. Antimicrob. Agents* **2009**, *33*, 421–426.

12. Liu, W.; Hua, J.; Zhou, J.; Zhang, H.; Zhu, H.; Cheng, Y.; Gust, R. Synthesis and *in vitro* antitumor activity of novel scopoletin derivatives. *Bioorg. Med. Chem. Lett.* **2012**, *22*, 5008–5012.

13. Iranshahi, M.; Askari, M.; Sahebkar, A.; Hadjipavlou-Litina, D. Evaluation of antioxidant, anti-inflammatory and lipoxygenase inhibitory activities of the prenylated coumarin umbelliprenin. *DARU J. Pharm. Sci.* **2009**, *17*, 99–103.

14. Li, M.; Li, J.; Liu, B.; Zhou, Y.; Li, X.; Xue, X.; Hou, Z.; Luo, X. Synthesis, crystal structures, and anti-drug-resistant *Staphylococcus aureus* activities of novel 4-hydroxycoumarin derivatives. *Eur. J. Pharmacol.* **2013**, *721*, 151–157.

15. Sheldrick, G.M. *SHELXL-97, Program for Solution Crystal Structure and Refinement*; University of Göttingen: Göttingen, Germany, 1997.

16. Frisch, M.J.; Trucks, G.W.; Schlegel, H.B.; Scuseria, G.E.; Robb, M.A.; Cheeseman, J.R.; Scalmani, G.; Barone, V.; Mennucci, B.; Petersson, G.A.; *et al*. *Gaussian 09*, Revision A.02, Gaussian, Inc.: Wallingford, CT, USA, 2009.

17. Hohenberg, P.; Kohn, W. Inhomogeneous Electron Gas. *Phys. Rev.* **1964**, *136*, B864–B871.

18. Kohn, W.; Sham, L.J. Self-Consistent Equations Including Exchange and Correlation Effects. *Phys. Rev.* **1965**, *140*, A1133–A1138.

19. Becke, A.D. Density-functional thermochemistry III. The role of exact exchange. *J. Chem. Phys.* **1993**, *98*, 5648–5652.

20. Lee, C.; Yang, W.; Parr. R.G. Development of the Colle-Salvetti correlation-energy formula into a functional of the electron density. *Phys. Rev. B* **1988**, *37*, 785–789.

21. Miehlich, B.; Savin, A.; Stoll, H.; Preuss, H. Results obtained with the correlation energy density functionals of becke and Lee, Yang and Parr. *Chem. Phys. Lett.* **1989**, *157*, 200–206.

22. Clinical and Laboratory Standards Institute (CLSI). *Performance Standards for Antimicrobial Susceptibility Testing: Nineteenth Informational Supplement M100-S19*; CLSI: Wayne, PA, USA, 2009.

23. Motyl, M.; Dorso, K.; Barrett, J. UNIT 13A.3 basic microbiological techniques used in antibacterial drug discovery. *Curr. Protoc. Pharmacol.* **2006**, doi:10.1002/0471141755.ph13a03s31.

24. Bassetti, M.; Merelli, M.; Temperoni, C.; Astilean, A. New antibiotics for bad bugs: Where are we? *Ann. Clin. Microbiol. Antimicrob.* **2013**, *12*, doi:10.1186/1476-0711-12-22.

25. Malani, P.N. Preventing postoperative *Staphylococcus aureus* infections. *JAMA* **2013**, *309*, 1408–1409.

26. Gordon, R.J.; Lowy, F.D. Pathogenesis of methicillin-resistant *Staphylococcus aureus* infection. *Clin. Infect. Dis.* **2008**, *46*, S350–S359.

Sample Availability: Samples of the compounds **1**–**5** are available from the authors.